DESIGN STUDY OF A COMPACT MEGAWATT CLASS FEL AMPLIFIER BASED ON THE VISA UNDULATOR*

T. Watanabe[#], D. Liu, J.B. Murphy, I. Pinayev, J. Rose, T. Shaftan, J. Skaritka, T. Tanabe, T. Tsang, X.J. Wang and L.H. Yu, BNL-NSLS, Upton, NY 11973, U.S.A.

S. Reiche,UCLA, L.A., CA 90024, U.S.A.

P. Sprangle, NRL, Washington D.C. 20375, U.S.A

Abstract

The design of a megawatt class FEL amplifier based on the strong focusing VISA undulator is presented in this report. The proposed FEL will operate at the 1 μm water window. Extensive simulations were performed to optimize an FEL amplifier based on the two-meter long VISA undulator which has a period of 1.8 cm and an undulator parameter K = 1.26. The betatron function inside the VISA undulator is about 30 cm. For an electron beam with a peak current ~1 kA and a normalized emittance of 5 mm-mrad, the FEL peak power can exceed 1 GW within the 2 m VISA undulator using a 5 kW peak power seed laser. Such a device can produce a megawatt of average power for a 700 MHz rep rate. The transverse distribution of the FEL radiation along the undulator, as well as after the undulator, is explored by numerical simulation. The FEL power density at 5 m downstream from the undulator is less than 100 kW/cm^2 for this MW-class FEL. We will also discuss the feasibility of an experimental demonstration of the laser seeded FEL amplifier based on the 2-m VISA undulator at the NSLS Source Development Lab (SDL).

INTRODUCTION

Tremendous progress has been made in high-average power FEL R&D recently when 10 kilowatts of average power was experimentally demonstrated in an FEL oscillator [1]. For the Navy's directed energy applications at least one MW of average power is required. A large intracavity power and a high power density on the cavity mirrors are major challenges for an FEL oscillator to achieve MW-class performance. Developments in accelerator technology, especially electron sources, make it feasible to explore single-pass FEL amplifiers for high average power applications [2]. A laser seeded FEL amplifier has the advantages of spectrum stability and operational simplicity. Two major challenges for a laser seeded FEL amplifier to achieve MW-class performance are efficiency and power density on the first guiding mirror.

Sprangle et al. proposed a novel scheme to avoid damage of the first mirror by employing optical guiding of the FEL light and a so-called "pinched e-beam" to generate a short Rayleigh range FEL [3]. In their scheme the e-beam is focused (pinched) in the last section of the undulator. The FEL light which is guided by the e-beam is then also pinched at the end of the undulator so that the Rayleigh length of the FEL is reduced significantly. We consider an alternative design of a MW-class laser seeded FEL amplifier based on a strong focusing undulator such as VISA [4]. A laser seeded FEL amplifier based on a strong focusing undulator has the advantages of a higher efficiency and a shorter Rayleigh length since the electron beam is tightly focused over the entire undulator. In this paper we present the design study of a laser seeded FEL amplifier using a two-meter VISA-type undulator. Extensive simulations were performed to optimize the FEL transverse distribution both inside and downstream of the undulator. GW FEL peak power (MW average) can be realized with reasonable electron beam parameters. The laser seeded FEL amplifier based the 2-m long VISA undulator could be experimentally studied at the NSLS SDL since most of the required hardware is available.

Table 1: VISA undulator and beam parameters

λ_u (cm)	1.8	E (MeV)	65
K_u	1.25	$\gamma\epsilon$ (mm-mrad)	2.0
β (cm)	30	I (A)	240
FODO (cm)	24	L_u (m)	2.0

TRANSVERSE DISTRIBUTION OF FEL LIGHT

The VISA undulator and the initial beam parameters used for the transverse distribution are summarized in Table 1. The strong focusing of the VISA undulator is provided by FODO cells built into the undulator [4]. For the small beam limit situation where the electron beam emittance is much smaller than the radiation wavelength, the rms radiation spot size can $\sigma_{x,y}$ be estimated using the following formula [5]:

$$\sigma_{x,y} = \sqrt{\frac{\lambda_r}{4\pi} 2L_G} , \qquad (1)$$

$$L_G^{-1} = \frac{4\pi}{\lambda_u} \frac{3^{3/4}}{2} \sqrt{\frac{I}{\gamma I_A} \frac{K^2[JJ]^2}{\left(1 + K^2/2\right)}} , \qquad (2)$$

where λ_r is the radiation wavelength, λ_u the undulator period, γ the electron energy in units of its rest mass, I_A the Alfven current, K the undulator parameter, and [JJ] the correlation for the longitudinal oscillation of electrons in a planar wiggler. Here the gain length L_G is obtained for the case that the radiation mode size is larger than the

electron beam size. Genesis1.3, a 3-D computer code, was used to study the FEL power and spot size evolution inside the undulator. Figure 1 represents the rms radiation size in $r = \sqrt{x^2 + y^2}$ along undulator for the seed laser peak power of 10 kW with different seed laser spot sizes. Two of the three seed laser sizes are chosen so that the filling factors, i.e., the ratio of the e-beam to the radiation cross-section area, are 1.0 (red curve in Fig. 1) and 0.5 (blue) at the entrance of the undulator. The third choice is that the seed laser spot size is the same as the FEL eigenmode (black). Here the rms electron beam size is oscillating from 60 to 160 μm, which is smaller than the radiation size. In all the cases, the radiation converged into the FEL eigenmode. Note that the radiation size in x (or y) based on Eq.(1) is 150 μm, whereas the size in Figure 1 is 300 μm in r, which corresponds to 212 μm in x (or y). The difference could be accounted for when 3-D effects are taken into consideration.
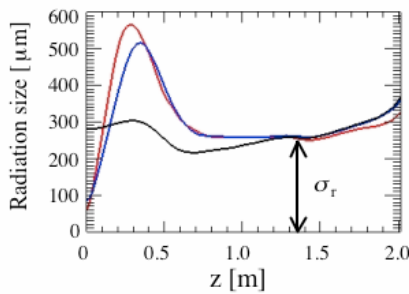
Figure 1: RMS radiation size along undulator for seed power of 10 kW. Red curve is for filling factor of 1.0, blue for filling factor of 0.5, and black for the same input size as the FEL eigenmode at the entrance of the undulator.

The FEL output power and rms beam size in r along the undulator are plotted in Fig. 2 for seed laser peak powers of 10, 50 and 100 kW. When the seed laser power is increased, the FEL reaches saturation earlier. Figure 2(b) shows that the rms radiation size starts increasing once the FEL reaches saturation. Figure 3 illustrates the two-dimensional FEL profile at the exit of the undulator. Note that the core radiation size for the 100 kW input is smaller than that with 10 kW and there is a satellite distribution in the 100 KW case. The increase in the rms size observed in Fig. 2(b) is dominated by the leakage of radiation due to the loss of gain guiding. Huang and Kim pointed out that the FWHM size is preserved while the rms size gets larger after saturation [6], with which agrees with our numerical simulation.

The evolution of the FEL radiation downstream beyond the undulator is determined not only by the radiation size (amplitude) at the undulator exit but also the phase. The propagation of the FEL pulse is simulated using the Fresnel free space propagator as given below [7],

$$u(x, y) = \int_S K(\theta) U(x, y) \frac{\exp(ikr)}{i\lambda r} dx dy , \quad (3)$$

$$K(\theta) = \frac{1 + \cos\theta}{2} , \quad (4)$$

where $u(x, y)$ is the downstream distribution, $K(\theta)$ is the directivity of the secondary wavelet, $U(x, y)$ is the distribution at the source, k is the wavenumber, λ is the wavelength and r and θ are the distance and angle between a source point and an observation point.

Figure 4 displays the FEL transverse distributions at 10 meters from the undulator exit for two input seed powers. One of the most interesting results from Figure 4 is that the far field FEL distribution is quite significantly different from the near field; a lower seed laser power produces a smooth and large spot size in the far field. This shows that the seed laser power can be used to control the FEL saturation and hence the transverse distribution in the far field.
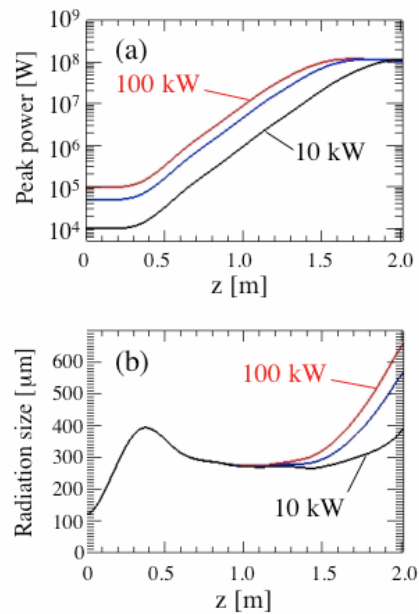
Figure 2: (a) Gain curve for three different input powers and (b) corresponding radiation beam size (rms).
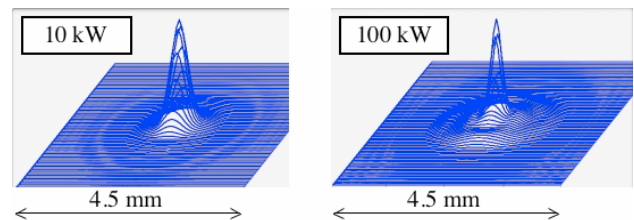
Figure 3: FEL radiation profiles at the exit of the undulator for two different input seed powers.
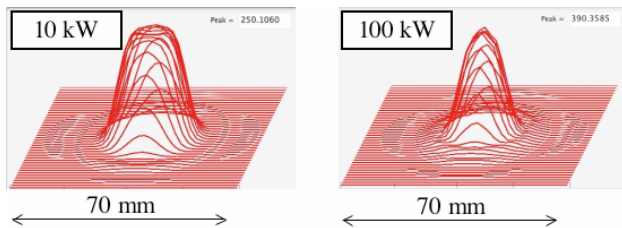
Figure 4: FEL radiation profiles at 10 m downstream for two different input laser seed powers.

An increase of the e-beam peak current will shorten the FEL gain length, increase the saturated power and also enhance the optical guiding [3]. We investigated the effects of the electron beam peak current on the FEL transverse distribution: the FEL saturates at 1.9 m for a peak current of 240 A and at 1.2 m for 1 kA. The FEL distribution at the undulator exit in each case did not show significant difference with those in Figure 3 except for minor differences in size and satellites. However the distribution at 10 m downstream for the 1 kA beam exhibits complex structure (Fig.5) including a hot spot. To avoid a hot spot in the far field, deep saturation should be avoided.
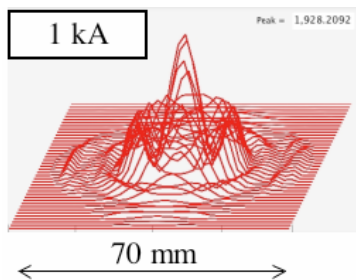
Figure 5: FEL distribution at 10 m with 1 kA peak current and 10 kW input power.

The above studies have shown the importance of the far field distribution of the FEL pulse for high average power applications. Figure 6 is a typical far-field distribution originating from a specific position in each regime inside the undulator. The distributions in Fig. 6 were calculated by GENESIS1.3. In Figure 6 we can see the following behaviors: (a) the input seed laser is assumed to have an ideal Gaussian distribution, (b) in the lethargy regime higher-order spatial modes have stronger diffraction, (c) in the exponential gain regime the higher-order modes are eliminated by diffraction and (d) the appearance of satellites after saturation. Once the FEL light exits the undulator and does not interact with e-beam any longer, the far-field distribution is preserved.
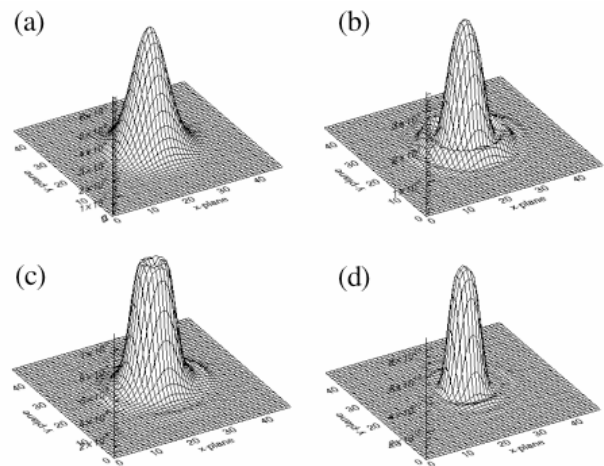
Figure 6: Evolution of the far-field FEL distribution calculated by GENESIS1.3. (a) input seed laser, (b) lethargy regime, (c) exponential gain regime, (d) after saturation.

GW PEAK POWER GENERATION

For a 1.4 ps FEL pulse and a linac repetition rate of 700 MHz, the FEL duty factor is 0.1%. To realize a MW-class average power performance, the FEL peak power of 1 GW is required. One GW peak power can be achieved either by increasing the e-beam power or by increasing the Pierce parameter ρ, since $P_{out} \approx \rho P_e$, where P_{out} is the output power and P_e is the e-beam power. For the 2-m long VISA undulator we are considering the electron energy is fixed to be 65 MeV by the output wavelength (1 µm) and the VISA undulator parameter (K=1.26). The betatron function is optimized to obtain matching with the FODO focusing of the VISA undulator. As such the electron beam peak current and the emittance are the two parameters that can be explored to increase the FEL output power. When the emittance is changed, the input beam size is changed in order to maintain proper matching of the betatron function. Therefore the change in emittance does not influence beam matching, but the filling factor is affected.

Figure 7 shows two sets of electron beam parameters that generate 1 GW output. The red curve in Fig. 7 was obtained for a normalized emittance of 2 mm-mrad and a peak current of 600 A, while the blue curve is for 5 mm-mrad and 1.1 kA. The input power of the seed laser was adjusted so that the FEL saturated within 2 meters but not deeply saturated to avoid distortion of the FEL profile. The seed laser peak power of 5 kW was employed for both sets of beam parameters in this study. The 5 kW peak power of the seed laser corresponds to 5 W average power, such a laser is readily available commercially.
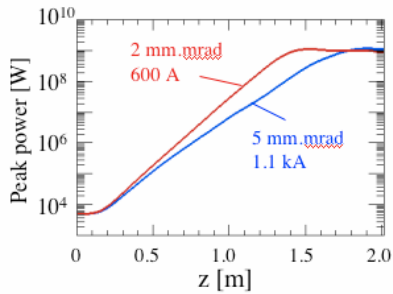
Figure 7: FEL radiation power along the undulator for a seed laser of 5 kW.

The optimized FEL profiles at the exit of the undulator and at 5 m downstream are shown in Figure 8(a) and (b), respectively. In Figure 8(a), no significant satellite is visible, which means that all the FEL radiation power is concentrated in the central peak. Hence, there will be no critical power loss as the light propagates. In Figure 8(b), the profile more closely resembles a flat-top, which is advantageous for avoiding damage to the guiding optics. Since the peak-to-peak size of the profile in Figure 8(b) is 3 cm, the FEL power density on a 45° mirror placed at 5 m away from the undulator is,

$$\frac{10^3\,[\text{kW}]}{\sqrt{2}\times\pi\times(3/2)^2\,[\text{cm}^2]} \approx 100\,[\text{kW}/\text{cm}^2]. \qquad (5)$$

This shows that, a compact (7 m) FEL based on the VISA undulator is capable of generating a MW-class FEL with power density below the damage threshold at the first guiding optics. Table 2 summarizes the undulator and beam parameters for the MW-class FEL based on the 2-m VISA undulator.

CONCLUSION

A compact MW-class FEL amplifier was designed by using the computer code GENESIS1.3. The study shows that the FEL amplifier using the 2 m VISA undulator is capable of producing a peak power of 1 GW, which corresponding to an average power of 1 MW for a 700 MHz linac. The e-beam and seed laser parameters are achievable in a practical experiment. The evolution of the FEL light distribution inside and downstream of the undulator was evaluated. The FEL light distribution can be optimized by avoiding deep saturation and the FEL intensity at 5 m downstream of the undulator can be below the damage threshold of the reflective optics. We are now proposing to perform a proof of principle experiment at the SDL using the existing 2-m VISA undulator at the NSLS.
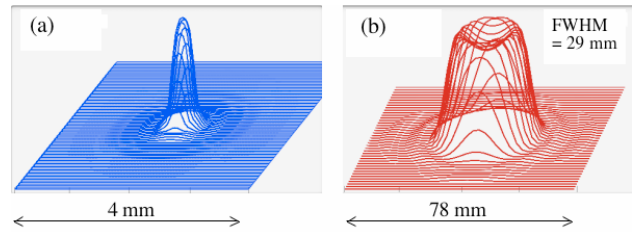
Figure 8: Optimized FEL profile (a) at exit of the undulator and (b) 5 meters downstream.

Table 2: Parameters for a compact MW FEL amplifier

Undulator		e-beam	
K	1.26	Energy	65 MeV
Period	1.8 cm	Ene. spread	0.05%
FODO	33.3 T/m	e-beam size	86, 60 μm
	9 cm	Emittance	5 mm-mrad
Drift space	3.6 cm	Peak current	1.1 kA
# of periods	110		
Total length	2 m	**Seed laser**	
		wavelength	1.0 μm
		input power	5 kW
		Rayleigh length	0.39 m

REFERENCES

[1] S. Benson et al, FEL2004 Proceedings, 229 (2004).
[2] D.C. Nguyen and H.P. Freund, NIM A507, 120 (2003).
[3] P. Sprangle et al, IEEE J. Quantum Electronics, 40 1739 (2004).
[4] R. Carr et al, PRSTAB, Vol. 4, 122402 (2001).
[5] Z. Huang, SLAC-PUB-11450, August 2005, to be published in the proceedings of FEL2005 (2005).
[6] Z. Huang & K.J. Kim, NIM A483, 504 (2002).
[7] E. Hecht & A. Zajac, Optics, Addison Wesley (1997).
[8] A. Murokh et al, PRE 67, 066501 (2003).